CH_3^+ Is the Most Trivial Carbocation, but Are Its Heavier Congeners Just Lookalikes?

Jürgen Kapp, Peter R. Schreiner,† and Paul v. R. Schleyer*

Contribution from the Computer Chemistry Center, Institut für Organische Chemie, Universität Erlangen-Nürnberg, Henkestrasse 42, D-91054 Erlangen, Germany

Received July 3, 1996[⊗]

Abstract: While the strongly bound D_{3h} AH_3^+ cations are favored energetically for CH_3^+ and SiH_3^+, C_s $HA^+\cdots H_2$ complexes are computed to be the global minima for A = Sn and Pb. The structures, relative energies, and dissociation limits (D_o) of the AH_3^+ cations (A = C, Si, Ge, Sn, and Pb) were studied at the Becke3LYP density functional level [6-311++G(2d,2p) basis sets for C, Si, and Ge, (quasi)relativistic effective core potentials with TZ+2P valence basis sets for Sn and Pb]. The SiH_3^+ potential energy surface computed for calibration at the CCSD(T) level is in very good quantitative agreement with the Becke3LYP results. The $AH_3^+ \rightarrow HA^+\cdots H_2$ rearrangement illustrates the rare case where *two* transition states are connected directly (one high-lying, 45−58 kcal mol^{-1} vs D_{3h} AH_3^+, and one lower in energy, 0−37 kcal mol^{-1}) without an intervening minimum. Due to the appreciable D_o values for both the AH_3^+ and the $HA^+\cdots H_2$ species, they should be experimentally verifiable.

Introduction

Small, seemingly familiar molecules may have uncharted features, particularly when the heavier main group elements are involved.[1] Surprisingly, the nature of the AH_3^+ cations (A = Si, Ge, Sn, and Pb) has not been explored in detail. As a part of his examination of the group 14 $A_2H_5^+$ polymorphs, Trinquier computed the entire set of group 14 AH_3^+ cations,[1a] but only in D_{3h} symmetry, as well as the monovalent AH^+ ions (which also are pertinent to the present study). While the experimental heat of formation of SiH_3^+ is available, no such data exist for GeH_3^+. We have found no experimental report even of the detection of SnH_3^+ and PbH_3^+. In contrast, the literature on CH_3^+ is vast,[2] and there are several studies on the silicon analog SiH_3^+.[3] Curtiss and Pople have established the theoretical thermochemistry of the silicon hydrides and their ions;[4] Raghavachari has explored the potential energy surfaces of various ions containing two or more silicon atoms.[5] However, the few theoretical papers on GeH_3^+ cations are concerned with other topics.[6]

Understandably, the D_{3h} geometries of the AH_3^+ cations have been taken for granted, since such structures are expected to follow the Walsh rules for six valence electron species. However, the trend toward lower oxidation numbers increases down group 14, and several inorganic Pb(IV) compounds are not stable thermodynamically with respect to dissociation.[7] For some A_nH_m species, neutral as well as cationic, complexes between an A_nH_{m-2} fragment and H_2 are minima.[5,6,8] Therefore, it is possible that the "trivial" AH_3^+ group 14 metal ions might not prefer classical D_{3h} structures but rather $HA^+\cdots H_2$ complexes. For example, such an $HC^+\cdots H_2$ complex was found for CH_3^+ at the HF/3-21G level of theory.[9] However, this stationary point was an artifact and collapsed to the classical D_{3h} geometry after optimization at all higher levels.

We now report a density functional theory (DFT) and high-level *ab initio* investigation on the heavier congeners of the methyl cation. The results are surprising: two minima could be located on the PES of the heavier AH_3^+ cations. Moreover, there are two interconnecting transition states, which pass directly from one to another, rather than via an intervening local minimum. These features reveal that the heavy metal AH_3^+ ions are only "seemingly related" to CH_3^+!

Computational Details

All structures were optimized at the Becke3LYP DFT level[10] using the GAUSSIAN 94 program.[11] Frequency calculations confirmed the nature of the stationary points.[12] The standard 6-311++G(2d,2p) basis set was employed for H, C, Si, and Ge.[13] For tin and lead,[14] the (quasi)-relativistic pseudopotentials of Stoll *et al.* (TZ+2P valence basis) were used.[15] For comparison and calibration, we also optimized some of the SiH_3^+ structures at the CCSD[16] and CCSD(T)[17] levels using a TZ2P

† Current address: Institut für Organische Chemie, Universität Göttingen, Tammannstr. 2, D-37077 Göttingen, Germany.

⊗ Abstract published in *Advance ACS Abstracts,* November 15, 1996.

(1) (a) Trinquier, G. *J. Am. Chem. Soc.* **1992**, *114*, 6807. (b) Trinquier, G. *J. Chem. Soc., Faraday Trans.* **1993**, *89*, 775. (c) Palágyi, Z.; Schaefer, H. F.; Kapuy, E. *J. Am. Chem. Soc.* **1993**, *115*, 6901. (d) Trinquier, G.; Malrieu, J.-P. *J. Am. Chem. Soc.* **1991**, *113*, 8634. (e) Trinquier, G. *J. Am. Chem. Soc.* **1991**, *113*, 144.

(2) (a) Lias, S. G.; Bartmess, J. E.; Liebman, J. F.; Holmes, J. L.; Levin, R. D.; Mallard, W. G. *J. Phys. Chem. Ref. Data* 1988, Suppl 1. (b) Olah, G. A., Schleyer, P. v. R, Eds. *Carbonium Ions*; Wiley: New York, 1976; Vols. I-V. (c) Vogel, P. *Carbocation Chemistry*; Elsevier: Amsterdam, 1985. (d) Hanack, M., Ed. *Houben-Weyl, Methoden der Organischen Chemie*; Thieme: Stuttgart, 1990; Vol. E19c. (e) Saunders, M.; Jiménez-Vázquez, H. A. *Chem. Rev.* **1991**, *91*, 375.

(3) (a) Hu, C.-H.; Shen, M.; Schaefer, H. F. *Chem. Phys. Lett.* **1992**, *190*, 543. (b) Hu, C.-H.; Schreiner, P. R.; Schleyer, P. v. R.; Schaefer; H. F. *J. Phys. Chem.* **1994**, *98*, 5040 and references cited therein.

(4) Lucas, D. J.; Curtiss, L. A.; Pople, J. A. *J. Chem. Phys.* **1993**, *99*, 6697 and references therein.

(5) (a) Raghavachari, K. *J. Chem. Phys.* **1991**, *95*, 7373. (b) Raghavachari, K. *Ibid.* **1992**, *96*, 4440.

(6) (a) Schreiner, P. R.; Schaefer, H. F.; Schleyer, P. v. R. Group IV Cation Dihydrogen Gas Phase Complexes and Their Neutral Analogs. Theoretical Considerations. In *Advances in Gas Phase Ion Chemistry*; Adams, N., Babcock, L. M., Eds.; JAI Press Inc.: London, England, 1996; Vol. 2. (b) Schreiner, P. R.; Schleyer, P. v. R.; Schaefer, H. F. *J. Chem. Phys.* **1994**, *101*, 2141. (c) Archibong, E. F.; Schreiner, P. R.; Leszcynski, J.; Schleyer, P.v. R.; Schaefer, H. F.; Sullivan, R. *J. Chem. Phys.* **1995**, *102*, 3667.

(7) (a) Cotton, F. A.; Wilkinson, G. *Advanced Inorganic Chemistry*, 5th ed.; Wiley: New York, 1988. (b) Huheey, J. E. *Inorganic Chemistry*, 3rd ed.; Harper: Cambridge, MA, 1983. (c) Greenwood, N. N.; Earnshaw, A. *Chemistry of the Elements*; Pergamon Press: Oxford, 1984.

(8) (a) Gordon, M. S.; Gano, D. R.; Binkley, J. S.; Frisch, M. J. *J. Am. Chem. Soc.* **1986**, *108*, 2191. (b) Su, M.-D.; Schlegel, H. B. *J. Phys. Chem.* **1993**, *97*, 9981. (c) Nachtigall, P.; Jordan, K. D.; Smith, A.; Jónsson, H. *J. Chem. Phys.* **1996**, *104*, 148.

(9) Raghavachari, K.; Whiteside, R. A.; Pople, J. A.; Schleyer, P. v. R. *J. Am. Chem. Soc.* **1981**, *103*, 5649.

S0002-7863(96)02275-5 CCC: $12.00

Table 1. AH_3^+ Relative Energies and Geometries (kcal mol^{-1}, Å, deg)[h] [at B3LYP with 6−311++G(2d,2p) Basis Sets for H, C, Si, and Ge and Quasirelativistiv Effective Core Potentials (ECP) (TZ+2P Valence Basis) for Sn and Pb]

isomer	energy[a]	AH	AH_m	AH_s	H_mH_s	H_sH_s	H_2[b]	A···H_2[c]	$\angle H_mAH_s$	$\angle H_sH_mH_s$
C D_{3h}	0.0	1.091								
$^+CH\cdots H_2$	128.8	1.145					0.749	3.074[d]		
$D_o(AH_3^+)$[e]	130.7	1.137								
Si D_{3h}	0.0	1.468								
TS1[f]	57.8		1.611	1.491	1.722	2.751			67.3	106.0
TS2	37.3		1.678	1.613	1.115	2.055			34.6	134.2
complex	27.1	1.514					0.782	1.983		
$D_o(AH_3^+)$[e]	34.7									
$D_o(HA^+\cdots H_2)$[g]	7.6									
Ge D_{3h}	0.0	1.524								
TS1	51.3		1.688	1.540	1.817	2.862			68.3	103.9
TS2	24.8		1.768	1.712	1.112	2.075			37.2	137.9
complex	10.0	1.591					0.773	2.121		
$D_o(AH_3^+)$[e]	16.3									
$D_o(HA^+\cdots H_2)$[g]	6.3									
Sn D_{3h}	0.0	1.689								
TS1	52.9		1.894	1.707	1.978	3.129			66.4	104.5
TS2	15.7		1.959	1.938	1.093	2.086			32.6	145.4
complex	−5.2	1.765					0.759	2.486		
$D_o(AH_3^+)$[e]	−2.3									
$D_o(HA^+\cdots H_2)$[g]	2.9									
n-Pb D_{3h}	0.0	1.784								
TS1	54.9		2.005	1.989	1.809	3.213			62.6	107.7
TS2	20.1		2.047	2.034	1.087	2.090			30.9	147.8
complex	−3.0	1.852					0.755	2.666		
$D_o(AH_3^+)$[e]	−2.3									
$D_o(HA^+\cdots H_2)$[g]	0.8									
Pb D_{3h}	0.0	1.719								
TS1	44.7		2.085	1.947	1.733	3.230			68.7	101.5
TS2	−0.3		2.017	2.012	1.086	2.089			36.3	148.2
complex	−23.3	1.817					0.756	2.619		
$D_o(AH_3^+)$[e]	−22.2									
$D_o(HA^+\cdots H_2)$[g]	1.1									

[a] Relative energies including ZPVE (=D_o); see the text. [b] H−H distance of the side-on ligand. Free H_2: 0.743 Å. [c] Distance between the H_2 midpoint and A; see Figure 1. [d] C−H···H_2 distance: 1.929 Å. [e] $AH_3^+ \rightarrow {}^+AH + H_2$. [f] Relative energy according to the CCSD(T)/TZ2P optimization (including Becke3LYP ZPVE): 61.1 kcal mol^{-1}. [g] $HA^+\cdots H_2 \rightarrow {}^+AH + H_2$. [h] See Figure 1. n-Pb refers to computing lead with a nonrelativistic ECP.

basis set.[18] The lowest core orbital was kept frozen, and the highest virtual orbital was deleted in the coupled cluster procedures. In addition, CCSD(T) single-point calculations were performed on the Becke3LYP optimized AH_3^+ (A = Ge, Sn, Pb) minima to evaluate the quality of the relative DFT energies.

To quantify the magnitude of relativistic effects,[19] the PbH_3^+ species also were computed with a nonrelativistic lead pseudopotential.[20] Atomic charges and Wiberg bond orders were obtained via Reed and Weinhold's natural bond orbital (NBO) analysis.[21] Figure 1 depicts all stationary points of the AH_3^+ PES (A = Si, Ge, Sn, and Pb). The relative energies of the isomers and geometries are given in Table 1; Table 2 presents natural atomic charges and Wiberg bond orders. In Table 3, relative energies of coupled cluster and DFT calculations are compared. As expected, the agreement is quite good;[22] thus, the Becke3LYP IR frequencies and rotational constants (Table 3) should be helpful in identifying the AH_3^+ isomers.[23]

Results and Discussion

Stationary Points. On the basis of the considerations given in the Introduction, we located planar $HA^+\cdots H_2$ side-on complexes as additional minima (besides the classical D_{3h}

(10) (a) Becke, A. D. *Phys. Rev.* **1988**, *A38*, 3098. (b) Becke, A. D. *J. Chem. Phys.* **1993**, *98*, 5648.

(11) *GAUSSIAN94*: Frisch, M. J.; Trucks, G. W.; Schlegel, H. B.; Gill, P. M. W.; Johnson, B. G.; Robb, M. A.; Cheeseman, J. R.; Keith, T.; Petersson, G. A.; Montgomery, J. A.; Raghavachari, K.; Al-Laham, M. A.; Zakrzewski, V. G.; Ortiz, J. V.; Foresman, J. B.; Cioslowski, J.; Stefanov, B. B.; Nanayakkara, A.; Challacombe, M.; Peng, C. Y.; Ayala, P. Y.; Chen, W.; Wong, M. W.; Andres, J. L.; Replogle, E. S.; Gomperts, R., Martin, R. L.; Fox, D. J.; Binkley, J. S.; Defrees, D. J.; Baker, J.; Stewart, J. P.; Head-Gordon, M.; Gonzalez, C.; Pople, J. A., Gaussian, Inc., Pittsburgh, PA, 1995.

(12) Hehre, W. J.; Radom, L.; Schleyer, P. v. R; Pople, J. A. *Ab Initio Molecular Orbital Theory*; J. Wiley & Sons: New York, 1986.

(13) (a) McLean, A. D.; Chandler, G. S. *J. Chem. Phys.* **1980**, *72*, 5639. (b) Krishnan, R.; Binkley, J. S.; Seeger, R.; Pople, J. A. *J. Chem. Phys.* **1980**, *72*, 650. (c) Frisch, M. J.; Pople, J. A.; Binkley, J. S. *J. Chem. Phys.* **1984**, *80*, 3265.

(14) Bergner, A.; Dolg, M.; Küchle, W.; Stoll, H.; Preuss, H. *Mol. Phys.* **1993**, *80*, 1431.

(15) d-polarization functions from Huzinaga, S., Ed. *Gaussian Basis Sets for Molecular Calculations*; Elsevier: New York, 1984.

(16) (a) Cizek, J. *Adv. Chem. Phys.* **1969**, *14*, 35. (b) Purvis, G. D.; Bartlett, R. J. *J. Chem. Phys.* **1982**, *76*, 1910. (c) Bartlett, R. J. *Annu. Rev. Phys. Chem.* **1981**, *32*, 359. (d) Bartlett, R. J. *J. Phys. Chem.* **1989**, *93*, 1697. (e) Scheiner, A. C.; Scuseria, G. E.; Rice, J. E.; Lee, T. J.; Schaefer, H. F. *J. Chem. Phys.* **1987**, *87*, 5361.

(17) (a) Raghavachari, K.; Trucks, G. W.; Pople, J. A.; Head-Gordon, M. *Chem. Phys. Lett.* **1989**, *157*, 479. (b) Bartlett, R. J.; Watts, J. D.; Kucharski, S. A.; Noga, J. *Chem. Phys. Lett.* **1990**, *165*, 513. (c) Scuseria, G. E. *Chem. Phys. Lett.* **1991**, *176*, 27.

(18) Si, (12s9p2d/6s5p2d); H, (5s2p/3s2p); $\alpha_d(Si) = 1.00, 0.25$), $\alpha_p(H) = 1.50, 0.375$. McLean, A. D.; Chandler, D. S. *J. Chem. Phys.* **1980**, *72*, 5639.

(19) (a) Schwerdtfeger, P.; Heath, G. A.; Dolg, M.; Bennett, M. A. *J. Am. Chem. Soc.* **1992**, *114*, 7518. (b) Kaupp, M.; Schleyer, P. v. R. *J. Am. Chem. Soc.* **1993**, *115*, 1061. (c) Wang, S. G.; Schwarz, W. H. E. *J. Mol. Struct.* **1995**, *338*, 347.

(20) Küchle, W.; Dolg, M.; Stoll, H.; Preuss, H. *Mol. Phys.* **1991**, *74*, 1245.

(21) (a) Reed, A. E.; Weinstock, R. B.; Weinhold, F. *J. Chem. Phys.* **1985**, *83*, 735. (b) Reed, A. E.; Weinhold, F. *J. Chem. Phys.* **1985**, *83*, 1736. (c) Reed, A. E.; Curtis, L. A.; Weinhold, F. *Chem. Rev.* **1988**, *88*, 899. (d) Reed, A. E.; Schleyer, P. v. R. *J. Am. Chem. Soc.* **1990**, *112*, 1434.

(22) Kapp, J.; Remko, M. Schleyer, P.v.R. *J. Am. Chem. Soc.* **1996**, *118*, 5745.

(23) Suggested Becke3LYP frequency scaling factor: 0.98. See: (a) Bauschlicher, C. W.; Partridge, H. *J. Chem. Phys.* **1995**, *103*, 1788. (b) Urban, J.; Schreiner, P. R.; Vacek, G.; Schleyer, P. v. R.; Huang, J.; Leszczynski, J. *Chem. Phys. Lett.*, in press.

Table 2. Natural Atomic Charges and Wiberg Bond Indices at Becke3LYP with 6−311++G(2d,2p) Basis Sets for H, C, Si, and Ge and Quasirelativistic Effective Core Potentials (TZ+2P Valence Basis) for Sn and Pb[e]

	charge					bond order						
isomer	A	H	H_m	H_s	H_2[a]	AH	AH_m	AH_s	H_mH_s	H_sH_s	A···H_2	H_2[b]
C D_{3h}	0.364	0.212				0.949						
$^+$CH···H_2	0.953	0.025			0.022	0.979						0.978
CH^+	0.993	0.007				1.001						
Si D_{3h}	1.376[c]	−0.125				0.928						
TS1	0.956		−0.059	0.051			0.892	0.844		0.103		
TS2	1.182		0.087	−0.134			0.355	0.537	0.319	0.132		
complex	1.230	−0.324			0.094	0.857					0.154	0.782
$^+$SiH	1.393	−0.393				0.848						
Ge D_{3h}	1.237[c]	−0.079				0.922						
TS1	0.896		−0.062	0.083			0.888	0.818		0.124		
TS2	1.188		0.082	−0.135			0.308	0.526	0.344	0.118		
complex	1.236	−0.318			0.083	0.874					0.120	0.866
$^+$GeH	1.378	−0.378				0.859						
Sn D_{3h}	1.603	−0.201				0.870						
TS1	1.225		−0.158	−0.033			0.831	0.773		0.156		
TS2	1.403		0.035	−0.219			0.187	0.424	0.407	0.127		
complex	1.414	−0.455			0.040	0.781					0.058	0.935
$^+$SnH	1.488	−0.488				0.762						
n-Pb D_{3h}	1.777[d]	−0.259				0.857						
TS1	1.369		−0.169	−0.100			0.794	0.752		0.150		
TS2	1.461		0.023	−0.242			0.163	0.395	0.419	0.134		
complex	1.468	−0.499			0.031	0.743					0.043	0.952
$^+$PbH	1.523	−0.523				0.727						
Pb D_{3h}	1.467[d]	−0.156				0.857						
TS1	1.144		−0.156	0.006			0.812	0.729		0.191		
TS2	1.395		0.034	−0.215			0.167	0.425	0.417	0.117		
complex	1.424	−0.458			0.034	0.782					0.044	0.951
$^+$PbH	1.485	−0.485				0.765						

[a] Corresponds to the $^+$HA ← H_2 charge transfer. [b] Bond order of the H_2 ligand. [c] Ge is more electronegative than Si; therefore, it is less capable of bearing a positive charge (see the text). [d] Relativity enhances the electron binding ability of the Pb 6s orbital (refs 19 and 34c). [e] n-Pb refers to computing lead with a nonrelativistic ECP.

Table 3. CCSD(T) and Becke3LYP Relative Energies,[a] Becke3LYP IR Frequencies[b] (cm^{-1}), IR Intensities (km mol^{-1}, in Parentheses), and Rotational Constants [*A*, *B*, *C*, GHz] of the AH_3^+ Minimum Structures (A = Si, Ge, Sn, and Pb) Calculated with 6-311++G(2d,2p) Basis Sets for H, C, Si, and Ge (Unless Noted Otherwise) and Quasirelativistic Effective Core Potentials (TZ+2P Valence Basis) for Sn and Pb

	Si			Ge		
	D_{3h}	side-on, C_s	$AH^+ + H_2$	D_{3h}	side-on, C_s	$AH^+ + H_2$
CCSD(T)	0.0	27.0	32.1[c,d]	0.0	12.1	16.5[e]
Becke3LYP	0.0	27.1	34.7	0.0	10.0	16.3
frequencies	842 (67.7)	539 (31.3)	2120 (71.4)	793 (19.7)	505 (20.3)	1961 (107.8)
	946 (60.1)	634 (0.6)		844 (34.4)	519 (0.2)	
	2265 (0.0)	739 (27.9)		2173 (0.0)	604 (20.1)	
	2347 (0.2)	933 (22.6)		2242 (0.1)	810 (16.1)	
		2112 (66.8)			1955 (105.3)	
		3832 (118.6)[f]			3969 (157.2)[e]	
A	155.1052	207.0334	226.3479	143.8737	186.3126	200.4741
B	77.5526	67.9538		71.9437	56.7402	
C		51.1613			43.4943	

	Sn			Pb		
	D_{3h}	side-on, C_s	$AH^+ + H_2$	D_{3h}	side-on, C_s	$AH^+ + H_2$
CCSD(T)	0.0	−6.8	−2.5[e]	0.0	−28.4	−27.1[e]
Becke3LYP	0.0	−5.2	−2.3	0.0	−23.3	−22.2
frequencies	691[g]	367	1785	659	317[g]	1714
	719	381		715	337	
	1956	430		1876	360	
	1999	634		1944	593	
		1777			1694	
		4168[f]			4218[f]	
A	117.1449	156.0023	162.2478	113.0958	145.4554	151.7371
B	58.5725	40.8067		56.5479	36.6126	
C		32.3458			29.2501	

[a] All relative energies including Becke3LYP ZPVE. [b] B3LYP vibrational frequencies may be scaled by a factor of 0.98; see ref 23. [c] SiH_3^+ isomers: CCSD(T)/TZ2P optimizations; see the text. [d] Relative energies of the CCSD/TZ2P optimized SiH_3^+ minima: 0.0 (D_{3h}), 27.5 (side-on, C_s), and 31.9 ($HSi^+ + H_2$) kcal mol^{-1}, respectively. [e] CCSD(T) single-point energies on Becke3LYP optimized structures. [f] Free H_2 at Becke3LYP/6-311++G(2d,2p): IR frequency 4416 cm^{-1} (intensity 0.0); rotational constant 1816.2434 GHz. [g] IR intensities are not provided for effective core potential calculations (Sn, Pb).

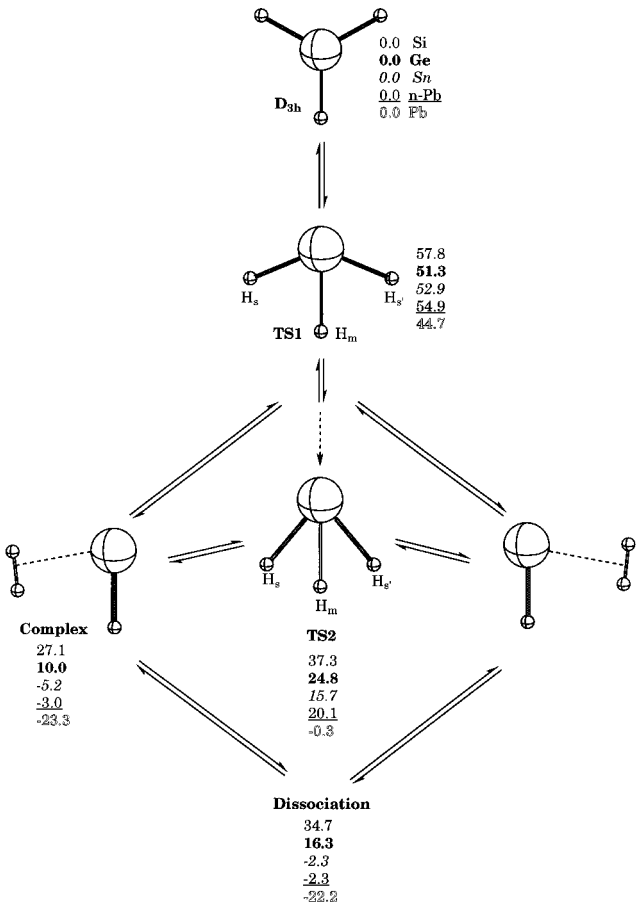

Figure 1. Schematic representation of the group 14 metal AH_3^+ potential energy surface. Relative energies (kcal mol^{-1}) (see also Table 1) at B3LYP utilizing a 6-311++G(2d,2p) basis for H, C, Si, and Ge and quasirelativistic effective core potentials (TZ+2P valence basis) for Sn and Pb. Key: silicon, light; **Germanium, bold**; *tin, italic*; nonrelativistic lead (n-Pb computed with a nonrelativistic effective core potential), underlined; lead, outlined numbers. The arrows between TS1 and TS2 indicate the bifurcation on the AH_3^+ PES (according to the intrinsic reaction coordinate (IRC) calculation; see text).

symmetric structures) for all heavier group 14 elements A = Si, Ge, Sn, and Pb (Figure 1).[24] We also were able to determine the general route connecting both these structures: in the first C_{2v} transition state (TS1) two A−H bonds are bent toward the third, "unchanged" A−H bond denoted as H_m ("middle", Figure 1). The negative eigenvector leads to a second stationary point (TS2) with C_{2v} symmetry. However, despite the short H···H distances, TS2 is not a minimum! Rather, TS2 is the transition state for hydrogen exchange between two equivalent, degenerate C_s symmetric side-on $HA^+\cdots H_2$ minima.

Hence, in going from the D_{3h} form to these C_s minima, the changes in geometry occur in discrete steps (Figure 1): first bending of the $H_s/H_{s'}$ ("side") hydrogens to TS1 and then their stretching in going to TS2. A transition state normally passes through a local minimum before reaching another transition state, but here the negative eigenvector of TS1 points toward TS2. This is possible due to the complimentary directions of the respective A−H stretching and H−A−H bending modes in the vector space along this part of the PES.[25,26] Such a bifurcation of the PES can be visualized as follows: in proceeding from TS1 toward TS2, the sides of the "saddle" fall off until the valley becomes a ridge. This ridge leads to TS2 without the intervention of an intermediate.

A Becke3LYP/6-311G** IRC calculation (in C_s symmetry) confirmed that TS1 connects the SiH_3^+ D_{3h} minimum with a nonminimum structure *approximately* resembling TS2.[27] Then the path connecting the two true minima (D_{3h} and C_s) leaves the TS1 "valley" until it becomes a ridge in TS2. Hence, the bifurcation of the AH_3^+ PES occurs shortly before TS2 is reached (Figure 1).[28] Thus, the reaction may avoid TS2, which only approximates the geometric changes along the $AH_3^+ \rightarrow HA^+\cdots H_2$ reaction path. The same should be true for the heavier group 14 AH_3^+ species.

Differences in Carbon vs the Metals. Investigations of the isoelectronic BH_3 system[29] and of the CH_3 radical[30] (the additional electron occupies the C 2p orbital perpendicular to the molecular plane and therefore is not involved) found almost no barrier (<1.0 kcal mol^{-1}) for the H_2 additions to BH and CH. There is a small barrier [5.6 kcal mol^{-1} at CCSD(T)TZ2P//CASSCF/TZ2P + thermal corrections)[31] for SiH insertion into H_2 in C_1 symmetry. However, we could not locate an addition pathway with a low barrier for the MH^+ (M = Si, Ge, Sn, and Pb) + H_2 insertion! The Becke3LYP activation energy of the D_{3h} SiH_3^+ decomposition (57.8 kcal mol^{-1}, TS1) is similar to the experimental (55.9 kcal mol^{-1})[32] and to the theoretical (56.9[8a] and 60[8b] kcal mol^{-1}) activation barriers for the silane dissociation into silylene SiH_2 and hydrogen H_2.[33] More sophisticated correlation treatments [CCSD and CCSD(T)] with a larger basis set (TZ2P) gave similar values for SiH_3^+ dissociation [Tables 1 and 3; $E^{\ddagger}$(TS1) = 61.1 and 60.1 kcal mol^{-1} at CCSD/TZ2P and CCSD(T)/TZ2P + ZPVE, respectively].

Recently, Nachtigall *et al.* investigated the H_2 elimination reactions from silanes using various DFT and *ab initio* methods.[8c] The SiH_4 dissociation activation energies ranged from 55.1 to 56.7 kcal mol^{-1}, while the transition state energy for the decomposition of disilane ($H_3Si-SiH_3 \rightarrow TS \rightarrow H_2 + H_3Si-SiH$) was found to be slightly lower, 52.0−53.2 kcal mol^{-1}. In contrast, Raghavachari computed the $Si_2H_5^+ \rightarrow H_2\cdots Si_2H_3^+$ barrier to be 33 kcal mol^{-1} (MP4SDTQ/6-311G**//MP2/6-31G**).[5]

Another difference between CH_3^+ and the group 14 AH_3^+ ions is that no side-on $HC^+\cdots H_2$ complex exists at Becke3LYP and the higher *ab initio* levels. Only a weakly bound van der Waals $^+C-H\cdots H_2$ complex (C_{2v}) could be located (Table 1). Unlike the heavier AH^+ species, the positive charge on CH^+ is on hydrogen. The electron population of CH_3^+ and the heavy group 14 cations also is different: both the carbon and the hydrogen atoms are positively charged, while the metal atoms

(24) HA^+ cation complexes with more than one dihydrogen ligand $[HA^+\cdots(H_2)_n]$, e.g., $HA^+\cdots(H_2)_2$ C_s, $HA^+\cdots(H_2)_3$ C_s, and $HA^+\cdots(H_2)_4$ C_{4v}, also can exist. However, their binding energies decrease with increasing *n*. For example, the $HGe^+\cdots(H_2)_n$ complexation energies at B3LYP/6-311++G(2d,2p) + ZPVE are 6.3, 5.2, 2.1, and 2.2 kcal mol^{-1} for the first, second, third, and fourth H_2 ligand, respectively.

(25) Cremer, D.; Svensson, P.; Kraka, E.; Ahlberg, P. *J. Am. Chem. Soc.* **1993**, *115*, 7445.
(26) Heidrich, D.; Kliesch, W.; Quapp, W. *Properties of Chemically Interesting Potential Energy Surfaces*; Springer-Verlag: Berlin, 1991; p 117.
(27) Note, however, that orthogonal trajectories (as used in the IRC algorithm) may not be suitable as reaction path models for the description of bifurcations: Valtazanos, P.; Ruedenberg, K. *Theor. Chim. Acta* **1986**, *69*, 281.
(28) For a recent discussion on determing bifurcation reaction paths, see: Taketsugu, T.; Tajima,N.; Hirao, K. *J. Chem. Phys.* **1996**, *105*, 1933.
(29) (a) Caldwell, N. J.; Rice, J. K.; Nelson, H. H.; Adams, G. F.; Page, M. *J. Chem. Phys.* **1990**, *93*, 479. (b) Schreiner, P. R.; Schleyer, P. v. R.; Schaefer, H. F. Unpublished results.
(30) Brooks, B. R., Schaefer, H. F. *J. Chem. Phys.* **1977**, *67*, 5146.
(31) Gordon, M. S.; Xie, Y.; Yamaguchi, Y.; Grev, R. S.; Schaefer, H. F. *J. Am. Chem. Soc.* **1993**, *115*, 1503.
(32) Moffat, H. K.; Jensen, K. F.; Carr, R. W. *J. Phys. Chem.* **1992**, *96*, 7695.
(33) For the dissociation barriers of the heavier MH_4 species see: Hein, T. A.; Thiel, W.; Lee, T. J. *J. Phys. Chem.* **1993**, *97*, 4381.

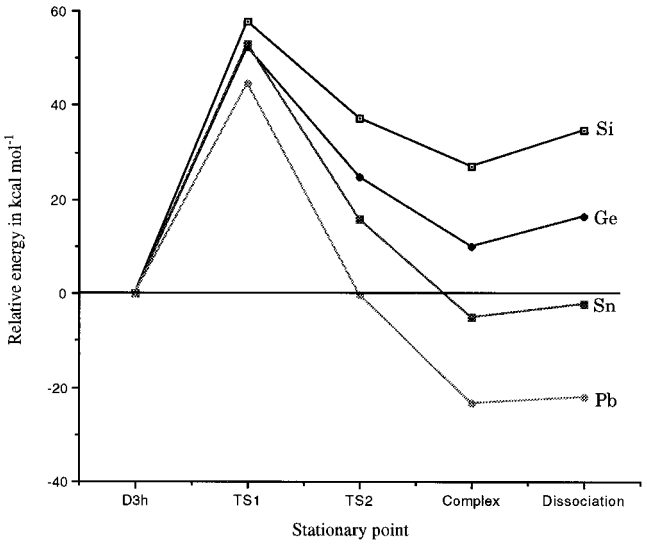

Figure 2. Diagrammatic presentation of the relative energies [kcal mol^{-1} (see also Table 1) at B3LYP utilizing a 6-311++G(2d,2p) basis for H, C, Si, and Ge and quasirelativistic effective core potentials (TZ+2P valence basis) for Sn and Pb] of the group 14 AH_3^+ stationary points: the D_{3h} minima, transition states 1 and 2, the C_s symmetric $HA^+\cdots H_2$ complexes, and the dissociated products AH^+ and H_2.

in AH_3^+ have positive charges greater than unity (Table 2). Electron density is transferred from the metals to the hydrogen atoms, depending on the isomer and the metal.

Relative Energies. The side-on complexes are high-lying local minima for SiH_3^+ and GeH_3^+, but they are the most stable isomers for SnH_3^+ and PbH_3^+ (relative energies vs the D_{3h} structure (kcal mol^{-1}): Si, 28; Ge, 10; Sn, −5; Pb, −23; Table 1 and Figure 2)! Comparison with the "nonrelativistic" PbH_3^+ isomers ("n-Pb") shows that the large preference for the lead side-on complex is due to relativistic effects, which stabilize the divalent state with a 6s lone pair on ^+Pb-H.[34] In contrast, the relative stabilities of these complexes toward dissociation into HA^+ and H_2 depend on the size of the metal: the silicon and germanium $HA^+\cdots H_2$ complexes are stabilized by 7 kcal mol^{-1}, but the tin and lead complexes are favored by only 1−3 kcal mol^{-1} over the separated fragments [$D_o(HA^+\cdots H_2)$, Tables 1 and 3].

The hydrogen exchange barrier (TS2) increases down group 14 from 10 (A = Si) to 15 (A = Ge) to 21−23 (A = Sn, Pb) kcal mol^{-1}, while the relative energy of TS1 vs the D_{3h} structure remains high (∼55 kcal mol^{-1} for Si, Ge, Sn, and nonrelativistic Pb). The lower 45 kcal mol^{-1} value for Pb indicates that the classical PbH_3^+ D_{3h} cation is destabilized by relativistic effects.

Electronic Structure. The natural population analysis (NPA) bond orders[21] and charges document the stronger covalent intramolecular interactions in the silicon and the germanium complexes and their TS2's relative to those in the corresponding tin and lead species (Table 2).

The $HA^+\cdots H_2$ side-on isomers are donor−acceptor complexes between the dihydrogen ligand (donor) and HA^+. The electron density transfer from the σ_{H-H} bond (as indicated by the group charge on the H_2 subunit, Table 2) to the empty p orbital at A (Si, Ge, Sn, and Pb) diminishes by about 50−60% in going from silicon and germanium to tin and lead. In addition to the size effect (see above), this interaction also depends on the electronegativity (EN) of the heavy atom. Note that Ge (2.0) has a higher EN than Si (1.7), leading to similar complexation energies for the latter two (Table 1), while the $HSn^+\cdots H_2$ and $HPb^+\cdots H_2$ interactions are significantly smaller. Consequently, the $Sn\cdots H_2$ and $Pb\cdots H_2$ bond orders are quite small (Table 2).

From a simple point of view, TS2 can be regarded as a very strong donor−acceptor complex between a formal H_3^- unit and a formal A^{2+} dication with an s lone pair (Figure 1). Strong electron donation from the occupied H_3^- orbitals occurs into two metal p orbitals. The Wiberg bond orders within the H_3^- unit increase considerably in going from germanium to tin (note the high H_mH_s bond orders), while the $A\cdots H_3$ interactions decrease (Table 2).

TS1 possesses an unusual MO structure: according to the NBO analysis,[21] only the $A-H_m$ bond has a distinctly localized orbital. The metal atom together with H_s and $H_{s'}$ forms a 3c-4e bond (including the metal s orbital and one p orbital).

Alternative Dissociation Mechanisms. Since TS1 is very high in energy, we tried to locate alternative pathways and computed two possibilities for the GeH_3^+ dissociation [Becke3LYP/6-311++G(2d,2p) level] as a model reaction: (1) stepwise homolytic cleavages of two of the Ge−H bonds ($AH_3^+ \rightarrow AH_2^+ + H^\bullet \rightarrow AH^+ + H_2$) and (2) H_2 abstraction via a route in C_{2v} symmetry. However, the products of the homolytic bond dissociation into $^\bullet GeH_2^+$ and $H^\bullet$ are about 33 kcal mol^{-1} higher in energy than TS1. Likewise, only very high energy nonstationary structures were found for the second alternative, H_2 abstraction in C_{2v} symmetry. When the C_{2v} symmetry constraints were removed, optimization of the H_2 abstraction pathway led to TS1. Strongly distorted GeH_3^+ starting geometries resulted in large $Ge\cdots H$ separations (i.e., homolytic Ge−H dissociation took place during the optimizations; $^\bullet GeH_2^+$ and $H^\bullet$ moieties, separated by several angstroms, were formed). Hence, we conclude that there is no energetically low-lying mechanistic alternative for AH_3^+ cation dissociation; the only route involves the high-lying transition state TS1.

Summary and Conclusions

Figure 2 predicts which AH_3^+ species should be experimentally accessible. Although the D_{3h} species only are metastable for A = Sn and Pb, all D_{3h} AH_3^+ forms should be observable due to the high barriers associated with H_2 loss (via TS1). The C_s side-on complexes are far less stable toward dissociation. In particular, they are unlikely to form from the D_{3h} isomers because the large thermal energy needed to overcome TS1 will lead to the separated products AH^+ and H_2 directly. The $HSi^+\cdots H_2$ and $HGe^+\cdots H_2$ complexes, prepared by association, appear to be most promising targets for experimental verification. Alternatively, divalent AR_2 compounds (R = alkyl, aryl, silyl, etc.) could be employed as precursors for the monovalent RA^+ cations.[24] $RA^+\cdots H_2$ side-on complexes might result from condensation with hydrogen.

Although the observation of the heavier AH_3^+ group 14 element cations may be difficult, their surprising structural and energetic features make them challenging experimental goals!

Acknowledgment. This research was supported by the Deutsche Forschungsgemeinschaft, by the Fonds der Chemischen Industrie, and by the Convex Computer Corp. J.K. acknowledges a grant from the Studienstiftung des Deutschen Volkes.

JA962275D

(34) For the effects of relativity on lead−hydrogen compounds see: (a) Dyall, K. G. *J. Chem. Phys.* **1992**, *96*, 1210. (b) Dolg, M.; Küchle, W.; Stoll, H.; Schwerdtfeger, P. *Mol. Phys.* **1991**, *74*, 1265. (c) Schwerdtfeger, P.; Silberbach, H.; Miehlich, B. *J. Chem. Phys.* **1989**, *90*, 762.